A Roughness-Based Matching Algorithm of Fractal Wavelet Coding for Side-Scan Sonar Images

FU-TAI WANG[1], C.-Y. JENNY LEE[2], HSIAO-WEN TIN[2] , SHAO-WEI LEU[3], CHAN-CHUAN WEN[4], and SHUN-HSYUNG CHANG[2*]

[1] Department of Electrical Engineering,
Hwa Hsia Institute of Technology
[2] Department of Microelectronics Engineering,
National Kaohsiung Marine University
[3] Department of Electrical Engineering,
National Taiwan Ocean University
[4] Department of Shipping Technology,
National Kaohsiung Marine University
Taiwan, R.O.C.

stephenshchang@mac.com http://60.249.147.181/oceaner/Main/index56.aspx

Abstract—This paper introduces an elaborative approach for indexing image feature and then applying those indices to a fractal-wavelet (FW) coding process. This approach reveals the texture similarities of an image by proposing a fractal dimension developed from the variance which measures the space filling degree of image roughness. The roughness-based FD was applied to the FW coding algorithm. Experiments were conducted using three side-scan sonar images of an undersea pipeline captured on the Polaris, Taiwan. The purpose of the experiment was to investigate the corresponding quality of the images in various configurations using two error criteria: the mean square error (MSE) and the peak signal-to-noise ratio (PSNR). The experimental results indicate that the roughness-based FD was adaptable to the FW coding matching process for approximating the experimental images.

Key-Words: Fractal dimension, Fractal-wavelet coding, Image approximation, Matching process, Roughness, Self-similarity

1 Introduction

Texture is regarded as a similarity grouped in an image. Efficiently extracting texture is a powerful method for classifying and identifying notable information in an area. The fractal dimension (FD) technique is a widely used texture analysis technique [1,2]. Roughness is a perceived image texture property, and is used to qualify image texture[3]. FD technique is suitable for estimating roughness and has been successfully applied to quantitatively measure texture [4,5]. The researchers were motivated to conduct this study by the observation that an FD expresses an image through surface stability, and the image roughness distribution can be used to describe the texture information derived from an image, thereby enabling the FD texture features to be extracted. The roughness-based FD value describes the distribution of image roughness, enabling the feasible FD representing texture features to be extracted from the images.

This study proposes a texture-based fractal-wavelet (FW) coding algorithm based on the roughness-based FD. The roughness-based FW algorithm uses the roughness-based FD to locate each range subtree for the optimal matched domain subtree according to the minimal texture similarity distances. The minimal similarity distance quantifies the degree of texture similarity between domain-range subtrees. Based on the roughness-based FW algorithm, conducting multiresolution frequency analysis on image texture is possible. Because the roughness-based FDs of images in different frequencies can be received on various scales, texture information can be acquired in a horizontal, vertical, and angular direction, which is seldom achieved by using other texture analysis methods. The proposed matching algorithm relies on texture similarity, thus enabling the roughness-based FD algorithm to effectively determine the appropriate domain subtrees to successfully approximate the range subtrees and preserve the image texture information of an image after encoding.

ISBN: 978-960-474-372-8

This study is organized as follows. Section II presents an overview of fractal techniques and the fractal-wavelet image coding scheme. Section III introduces the proposed wavelet-fractal coding matching algorithm. Section IV includes the experimental results and conclusions. The experimental results are discussed using the measurements of mean square error (MSE) and peak signal-to-noise ratio (PSNR). The final section presents a brief conclusion.

2 Fractal Image Coding and FW Coding

Fractal block coding is the most popular method among fractal technical which has been developed for decades since its first introduce in the early 1960 [6-8]. A drawback in fractal block coding is that to match a group of domain blocks to a range block is time consuming. Many researches have been proposed to improve the matching process by reducing domain pool such as [9, 10]. Fractal block coding and wavelets have also been combined first by Pentland and Horowitz [11] in the early 1990s. In 1998, Davis [12] published an important paper in which wavelets and fractal image coding were linked.

2.1 Fractal Block Coding

Fractal block coding is used to approximate an image based on the subblocks of that image. The following introduces the Jacquin fractal block coding theory.

Let I be a gray-level image. In fractal block coding, Image I is partitioned into N range blocks $R_i \subseteq I$, for i = 1, 2…, N, and M domain blocks $D_j \subseteq I$, for j = 1,2,…, M, where the size of each domain block is twice the size of each range block. To encode an image according to self-similarity, each range block locates the domain block in the domain pool most similar to itself. The location process is based on minimal MSE criteria. The search for the optimal matched domain block D_j is performed using local affine transformation w_i , such that $w_i : D_j \to R_i$, for i = 1,2, …, N and j = 1, 2, …, M. Theoretically, the union of the local affine transformations for all range blocks is the affine transformation τ for the entire image, as expressed in (1).

$$\tau = \bigcup_{i=1}^{N} w_i \tag{1}$$

In practice, each local affine transformation w_i is performed such that $R_i \approx w_i\left(D_j\right)$. Image encoding is achieved by first generating a fractal code for each range block R_i based on the optimal matched domain block D_j, and then storing the fractal code in the codebook. Fractal codes recorded in the codebook can later be used in the iterating range approximation process to restore the image.

2.2 Basics of FW Coding

Quadtree fractal coding, suggested by Fisher [13], is one of the most commonly applied hierarchical segmentation-based coding schemes and has been extensively studied [12,14]. Fisher's scheme suggested to locate the optimal matched domain subtrees to approximate the range subtrees using the proper affine transform, common scaling factors, and three fundamental coefficient trees—the horizontal, vertical, and diagonal trees. However, this restriction decreases image fidelity. Davis [12] provided a now widely used toolkit useful for implementing experiments.

Ghazel et al. [14] considered the coefficients of three subtrees independently in their FW coding scheme, which involves the selection of the optimal parent subtree, which minimizes the collage error measured using the MSE of the noiseless image. This ensures to obtain a successful collage-based matching criterion for getting noise-free image.

An iteration of the FW scaling and copying procedure produces a fixed point wavelet coefficient matrix that is an approximation of the original image. A small collage distance produces an accurate approximation [15]. The collage coding procedure used to produce the FW code is described as follows: First, consider a fixed set of parent-child level values. Then, for each unencoded child subtree, determine the parent subtree and the corresponding scaling coefficient to minimize the collage distance.

3 Roughness-based FW Algorithm

FD is a useful tool that can be used to measure the degree of roughness of a surface texture. Based on these concepts, this study proposes a roughness-based FD approach to measuring image roughness. The novel FD efficiently extracts roughness properties of an image to describe the texture of images.

The roughness-based FD is used to estimate domain-range matching in FW based on the relative degree of texture similarity. The smallest distance between the two roughness-based FD values of

ISBN: 978-960-474-372-8

subtrees in higher and lower frequency subbands must be calculated. The encoding is performed using an affine transformation defined by Jacquin [8]. Section 3.2 describes the roughness-based FW algorithm.

3.1 Roughness-based FD

The creation of the roughness-based FD was inspired by the allometric relationship between the number of roughness nodes and the compound path length. The roughness-based FD clusters the image roughness and subsequently structures to a compound based on the two-connectivity rule. The FD of the compound was derived according to the structure, which was quantified using the Horton-Strahler order scheme [16]. Shannon entropy was introduced when integrating the FDs of the compound into an FD of an image. The entropy reflected the roughness contribution of the same type of compounds to the image. The derived FD summarizes the image roughness complexity as a single numerical value.

Three steps are proposed to obtain the roughness-based FD.

1. Image Roughness Extraction

Image roughness was defined as a descriptor of pixel value variation between pixels in a small neighborhood. A pixel was referred to as an image roughness when the current pixel value was greater than the maximum or less than the minimum of surrounding pixels. The surrounding pixels were those pixels that are adjacent to the current pixel in the vertical and horizontal directions, as shown in Fig. 1. This study groups image roughnesses that are adjacent to each other into a roughness cluster.

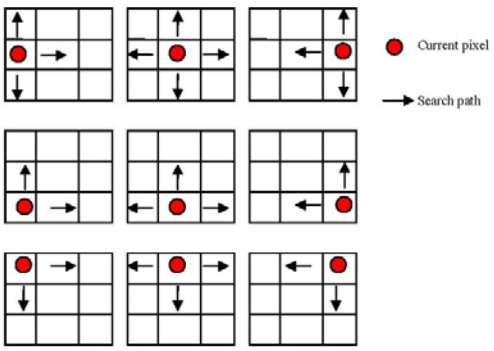

Fig. 1. Locating surrounded pixels

2. Calculating the FD for Each Compound

This study constructs a compound by structuring the image roughnesses in each cluster according to the two-connectivity rule. Let each image roughness have an order that defaults to one. Two adjacent image roughnesses construct a node. The node is called a roughness node and the order of this node is set to one order higher than the foundation. Two adjacent nodes of the same order construct a new roughness node. The order of the new node is set to one level higher than the foundation of the node. This process is repeated until all of the roughness nodes have been examined. The roughness compound is defined as a set of image roughnesses and roughness nodes, in which the nodes are constructed using the elements in the same set. The highest node order at the end of the node traversal process is assigned as the order of that compound. Consequently, the hierarchical structure of a compound is a binary tree.

This study derives an algorithm from the Horton laws [17] to compute the FD by considering two essential features: the number of roughness nodes and the roughness node path length.

The number of roughness nodes ratio, R_n, is defined as follows:

$$R_n = N_{od\_r+1} / N_{od\_r}, \quad (2)$$

where od_r is the order and N_{od_r} is the number of roughness nodes of order od_r.

The average path length ratio, R_L, is defined as follows:

$$R_L = L_{od\_r+1} / L_{od\_r}, \quad (3)$$

where L_{od_r} is the average path length of order od_r. The average path length of the roughness nodes of order i was defined as the total path length of those roughness nodes divided by the number of roughness nodes of order i.

If a compound contains N_1 roughness nodes, the number of second order roughness nodes is obtained as follows

$N_2 = N_1 \times R_n$.

If the structure of a compound is a symmetric binary tree, the number of roughness nodes in order k is calculated as follows:

$$N_k = N_1 \times R_n^{k-1}. \quad (4)$$

Consequently, the average path length in order k is calculated using (5).

$$L_k = L_1 \times R_L^{k-1} \quad (5)$$

Apply a logarithm transformation to both sides of (5).

$$\log L_k = \log\left(L_1 \times R_L^{k-1}\right)$$

$$\log L_k = \log L_1 + (k-1)\log R_L$$

$$k-1 = \left(\log L_k - \log L_1\right)/\log R_L$$

$$k-1 = \log\left(L_k / L_1\right)/\log R_L$$

ISBN: 978-960-474-372-8

Substitute $k-1=\left(\log L_k-\log L_1\right)/\log R_L$ into (4) to obtain

$$N_k = N_1 \times R_n^{\left(\log\left(L_k/L_1\right)/\log R_L\right)}.$$

Based on the Change-of-Base formula of the logarithm, $\log_b x = \log_a x/\log_a b$,

$$N_k = N_1 \times R_n^{\left(\log\left(L_k/L_1\right)/\log R_L\right)}$$
$$N_k = N_1 \times R_n^{\log_{R_L}\left(L_k/L_1\right)}.$$

Based on the logarithm formula $a^{\log b} = b^{\log a}$,

$$N_k = N_1 \times R_n^{\log_{R_L}\left(L_k/L_1\right)}$$
$$N_k = N_1 \times \left(L_k/L_1\right)^{\log_{R_L} R_n}.$$

Reapply the Change-of-Base formula of the logarithm.

$$N_k = N_1 \times \left(L_k/L_1\right)^{\left(\log R_n/\log R_L\right)}$$
$$N_k = N_1 \times L_1^{-\left(\log R_n/\log R_L\right)} \times L_k^{\log R_n/\log R_L}$$

Because $L_1^{-\left(\log R_n/\log R_L\right)}$ and N_1 are constant, let $c = N_1 \times L_1^{-\left(\log R_n/\log R_L\right)}$.

$$N_k = c \times L_k^{\left(\log R_n/\log R_L\right)} \quad (6)$$

(6), which represents the structure of the compound, is a power-law function and is similar to the FD measure $N(l) \propto l^{-D}$, which represents the Mandelbrot fractal relationship. These details are described in [6]. Therefore, the FD of a compound was defined as follows:

$$D = \log\left(R_n\right)/\log\left(R_L\right). \quad (7)$$

In practice, R_L is a constant, and the linear regression approach does not apply in calculating the FD. Therefore, the geometric mean was applied to calculate the average of R_n and subsequently applied to (7) to obtain the FD of the compound.

Although (7) has been derived to obtain the FD of a symmetric binary tree, Frontier suggested that the FD of a nonhomogeneous tree can be obtained by using the same algorithm applied to a symmetric binary tree [18]. Therefore, this study applies (7) to every compound, regardless of structure.

3. Calculating the FD of an Image.

The roughness-based FD classifies the compounds based on the order and number of image roughnesses. A set of classified compounds with a low presence frequency reflects the texture of that image. This study assigned Shannon entropy to the classified compounds based on information theory, in which entropy represents compound randomness. The study obtains the image FD by summing the products of compound FDs and compound entropies.

Assume that an image contains n sets of classified compounds $\{c_1, c_2, ..., c_n\}$. Therefore, the presence frequency of the ith (i = 1, 2,..., n) set of compounds in that image is described as (8),

$$P_i = n\_c_i/total\_n\_C, \quad (8)$$

where n_c_i is the number of the ith set of compounds, and $total\_n\_C$ is the total number of compounds in that image.

The information on the ith set of compounds with presence frequency P_i is expressed as $I\left(c_i\right) = -\log\left(P_i\right)$. The Shannon entropy assigned to the ith set of compounds is the product of P_i and $I\left(c_i\right)$. Therefore, the Shannon entropy for the ith set of compounds is $P_i \times \left(-\log P_i\right)$. These FDs of the compound were integrated to form an FD of image fE. fE is obtained by using (9)

$$fE = -\sum_{i=1}^{n} P_i \left(\log P_i\right) fD_i \quad (9)$$

where fD_i is the FD of the ith set of compounds obtained using (7). The derived FD summarizes the image roughness complexity as a single numerical value.

3.2 Roughness-based FW Coding Method

The proposed method estimates the domain-range matching based on the relative degree of texture similarity, as shown in Fig. 2. The range subtree was approximated by using the affine grayscale transformations of the domain subtrees.

ISBN: 978-960-474-372-8

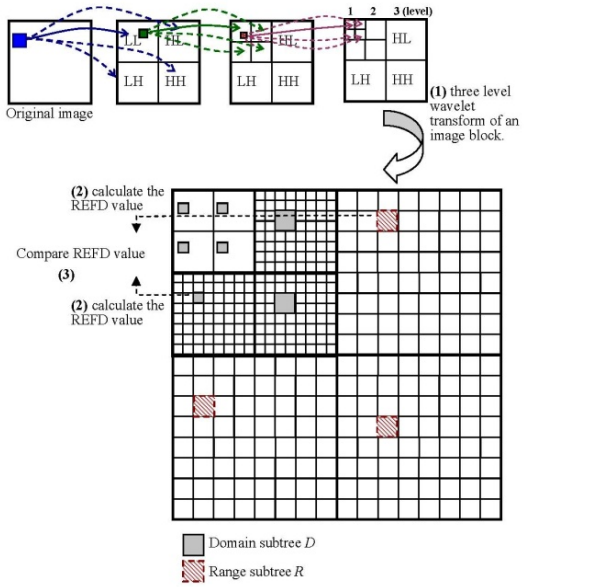

(1) Wavelet transform decomposes the image into two parts which respectively represent low frequency L and high frequency H, and then REFD and fractal block coding perform in the wavelet domain

(2) Obtain the sub-sampling domain block of resolution 2 in HL and calculate the REFD, and then compare to the REFD of the range block of resolution 1.

(3) If the differential of REFD value is the minimal, this domain block is selected as the best matched

Fig. 2. Illustration showing roughness-based FD works in finding the appropriated domain subtrees to match the range subtrees.

The image subtrees can be split into *n*-level decomposition by using a quadtree partitioning scheme. Each level includes one low-frequency subband and three high-frequency subbands from various directions. The collage error was used as a splitting criterion and the maximal splitting depth decreased to a limited number, depending on the image size and block size. Mapping the affine transformation domain subtree into the corresponding range subtree was described in [8]. The encoded parameters include the position of the domain tree and the scaling factor. The experiment in this study did not implement rotation and flipping in the affine transformation.

4 Experimental Results and Conclusion

4.1 Measuring Performance

The proposed method leads to an approximation of the original noise-free image. The performance evaluation is taken by using two well-defined error criteria, the MSE and PSNR.

$$MSE = \frac{1}{N \times M} \sum_{x=0}^{N-1} \sum_{y=0}^{M-1} \left(B(x,y) - A(x,y) \right)^2 \qquad (10)$$

where $A(x,y)$ is the gray value expression of original image A, and $B(x,y)$ is the gray value expression of decoded image B. The images are the same size as $N \times M$.

Generally, if the PSNR is sufficiently large, no humanly perceptible difference exists between the reconstruction and the original image.

$$PSNR = 10 \log_{10} \frac{I_{\max}^2}{MSE}, \qquad (11)$$

where $I_{\max}$ is the highest intensity pixel in the image [19], in which the intensity is 256 in gray images.

4.2 Experimental Results

The performance of the proposed roughness-based FW algorithm was evaluated. A classical comparison analysis was conducted based on the emulated noisy image. It was built by using a high-quality image as the original, adding Gaussian white noise of a given variance σ to the original image, and then using the denoising method to approximate the original image using the noisy image. Therefore, three side-scan sonar images of a pipeline, which were captured by the Polaris, Taiwan, were selected as the experimental objects, as shown in Fig. 3. They were enlarged to 2048 × 2048 pixels and transformed to an 8-bit gray image. Gaussian white noise (with zero mean and variance σ = 0.01) was then added to the original sonar image to create the noisy image. The roughness-based FW algorithm and a slightly modified generic FW scheme were used to reduce the noise in the noisy sonar images.

The proposed method was also compared with a generic FW compression algorithm introduced by Avanaki et al. [17]. Table 1 shows that the roughness-based FD produced more favorable FD values than the generic FW algorithm did.

4.3 Conclusion

An FW denoising alternative based on applying a texture analysis technique to the fractal matching process was proposed in this study. The performance of the roughness-based FW algorithm was demonstrated by applying it to a sonar image. The analysis of the results indicated that the novel algorithm based on texture similarities demonstrates the adaptability of the algorithm when images are denoised for a side-scan sonar.

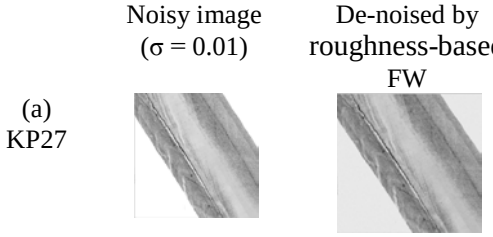

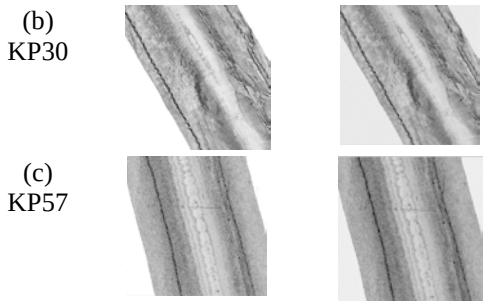

Fig. 3. De-noising effects for sonar image of the pipeline exposure and freespan taken by the Polaris

Table1. The MSE and PSNR values for the noisy sonar image after de-noising

		σ = 0.01			σ = 0.05			σ = 0.1		
		(a) KP27	(b) KP30	(c) KP57	(a) KP27	(b) KP30	(c) KP57	(a) KP27	(b) KP30	(c) KP57
Noisy image	MSE	40693	38852	34150	40712	38871	34168	40727	38886	34181
	PSNR	2.070	2.271	2.831	2.068	2.269	2.829	2.07	2.267	2.827
The proposed algorithm	MSE	151	229	187	297	358	270	503	553	396
	PSNR	26.37	24.57	25.45	23.43	22.63	23.86	21.15	20.74	22.18
FW coding [19]	MSE	40682	38851	34147	40683	38852	34148	40684	38853	34150
	PSNR	2.071	2.271	2.831	2.070	2.270	2.831	2.066	2.271	2.831

Acknowledgments

This work was supported by the National Science Council of Taiwan, R.O.C. under contract NSC 102-2221-E-146-004-.

References:

[1] B. B. Chaudhuri and N. Sarkar, "Texture segmentation using fractal dimension," IEEE Trans. Pattern Anal. Mach. Intell., Vol. 17, No. 1, 1995, pp.72-77.

[2] R. Dobrescu, M. Dobrescu, S. Mocanu, D. Popescu, "Malignant skin lesions detection based on texture and fractal image analysis," Proceedings of the 10th WSEAS International Conference on MULTIMEDIA SYSTEMS & SIGNAL PROCESSING (MUSP '10), 2010, pp21-26

[3] L.M. Linnett, D.R. Carmichael, S.J. Clarke, A.D. Tress, "Texture analysis of sidescan sonar data," *IEE Seminar on Texture analysis in radar and sonar*, 1993, pp. 2/1-2/6.

[4] H.-W. Tin, S.-W. Leu, F.-T. Wang, C.-C. Wen, and S.-H. Chang, "Denoising Algorithm Based on Fractal-Wavelet coding and its Application to Side-scan Sonar Image," *2013 International Symposium on Physics and Mechanics of New Materials and Underwater Applications (PHENMA 2013)*, 2013, pp. 30.

[5] H.-W. Tin, S.-W. Leu, C.-C. Wen, and S.-H. Chang, "An efficient sidescan sonar image denoising method based on a new roughness entropy fractal dimension," 2013 IEEE International Underwater Technology Symposium (UT), 2013, pp.1-5.

[6] B.B. Mandelbrot, *Fractal Geometry of Nature*, San Francisco, CA: Freeman ,1982.

[7] M.F. Barnsley, S. Demko, "Iterated function systems and global construction of fractals," *Proceedings of the Royal Society of London*, 1985, pp.243-275.

[8] A.E. Jacquin, "Image Coding Based on a Fractal Theory of Iterated Contractive Image Transformations," *IEEE Trans. Image Processing*, 1992, pp.18-30.

[9] H.-W. Tin, S.-W. Leu, and S.-H. Chang, "An PSO-based Approach to Speed up the Fractal Encoding", *International Journal of Mathematical Models and Methods in Applied Sciences*, 2012, Vol.6, pp. 499-506.

[10] H.-W. Tin, S.-W. Leu, H. Sasaki, and S.-H. Chang, "A Novel Fractal Block Coding Method by Using New Shape-Based Descriptor", *Applied Mathematics & Information Sciences*, 2014, Vol. 8, No. 2, pp. 849-855.

[11] A. Pentland and B. Horowitz, "A practical approach to fractal-based image compression, " *in Proc. Data Compression Conf., Snowbird, UT*, 1991, pp. 176-185.

[12] G.M. Davis, "A Wavelet-Based Analysis of Fractal Image Compression," *IEEE Trans. Image Processing*, 1998, Vol. 7, pp. 141-154.

[13] Y. Fisher, *Fractal Image Compression-Theory and Application*, NewYork: Springer Verlag, 1995.
[14] M. Ghazel, G. Freeman, and E. R. Vrscay, "Fractal-wavelet Image Denoising Revisited, " *IEEE Transactions on Image Processing*, Vol.15, 2006, pp. 2669-2675.
[15] J. Lu, Y. Zou, and Z. Ye , "Enhanced Fractal-Wavelet Image Denoising," *ISECS International Colloquium on Computing, Communication, Control, and Management (CCCM '08)* ,2008, pp. 115 – 119.
[16] Strahler, A. N., *Quantitative analysis of watershed geomorphology*, Am. Geophys. Union Trans., pp. 913-920, 1957.
[17] R. E. Horton, "Erosional development of streams and their drainage basins: hydrophysical approach to quantitative morphology," *Bull.Geol. Soc. Am.*, 1945, pp. 275-370.
[18] S. Frontier, "Applications of Fractal theory to Ecology, " *Legendre, P., Legendre, L. (Eds.), Developments in Numerical Ecology*, 1987, pp. 335-378.
[19] M.R.N. Avanaki, H. Ahmadinejad, R. Ebrahimpour, "Evaluation of Pure-Fractal and Wavelet-Fractal Compression Techniques," *International Journal on Graphics, Vision and Image Processing*, Vol. 9, Issue IV, 2009, pp. 41-47.